Retinal Fundus Features Hybrid Detection based on a Genetic Algorithm

Vitoantonio Bevilacqua Lucia Cariello Simona Cambò Domenico Daleno Giuseppe Mastronardi

DEE Polytechnic of Bari
Via Orabona, 4
70125 Bari, Italy
+39 080 5963252
mastrona@poliba.it

ABSTRACT
In this paper, an analysis of images of the retinal fundus by means of a combination of soft-computing techniques is carried out in order to extract from blood vessels their bifurcation and crossover points. These retinal features are unique for each individual and therefore they are useful for a successive process of personal identification. In particular, the implemented method is based on four steps. In the first step, a pre-processing of the input image by using, in sequence, several filters is carried out: the retinal image is processed by means of pixel to pixel elaboration algorithms to obtain a black and white image representing the template of retinal veins and arteries. In the second step, applying to the so obtained image a genetic algorithm, the edges' template is extracted. To this point, in the third step, the method continues with a skeleton process of the contours making use of an empirical algorithm. Finally, in the last step, the goal is caught up by characterising the searched points by means of a tracking algorithm.

Categories and Subject Descriptors
I.4.6 [**Image Processing and Computer Vision**]: Segmentation – *edge and feature detection.*

General Terms
Security, Measurement, Algorithms.

Keywords
Medical imaging, biometrics, identification points, retinal fundus, vessel bifurcation and crossover detection, genetic algorithm, edge detection, skeleton extraction, tracking algorithm.

1. INTRODUCTION
Biometric technology improves the accuracy which systems can identify individuals with. Personal identification involves a very large type of life situations and this is the reason for the high interest given, in the last years, to the biometric methods [7]. Biometric security technologies, in fact, are being incorporated into many applications for improving airport security, preventing business theft, strengthening our national borders, into travel documents, visas and in preventing ID theft.

This technology relies on measurements of physical characteristics unique to an individual such as fingerprints, facial features, retinal fundus, iris, hand geometry, or behavioural characteristics such as voice, handwritten signature. Since these characteristics are unique to each individual, biometrics are believed to effectively combat theft and fraud in a wide variety of industries and applications. One technology has emerged in the biometric area: *retinal recognition*. The retina, a layer of blood vessels located at the back of the eye, forms an identity card for the individual under investigation. In particular retinal recognition creates an "eye signature" from its vascular configuration and its artificial duplication is thought to be virtually impossible. For all these reasons, the retinal image offers a personal identification method of extreme high accuracy [8].

The retinal recognition process can be so summarised: the user looks at a green dot for a few seconds until the eye is sufficiently focused for a scanner to capture the blood vessel pattern. An area known as the fovea, located in the centre of the retina, is then scanned by an infrared beam. The retina pattern is captured, its features are extracted and then they are compared to previously-stored patterns for identification. If there is a match that meets a preset recognition threshold, the identification is accepted as valid [11].

This paper is dipped in this scenario. In fact this work is interposed between the image capture process and the comparison process: it consists of a method of features extraction. In other words a map of main bifurcation and crossover points are extracted from a retinal fundus image for a successive process of personal identification.

Several methods have been developed to detect retinal fundus blood vessels. In particular, the method described in this paper, derives inspiration from a technique existing in literature [1]. However, after a first common step, the two methods take completely different directions to reach the same goal. In fact in both techniques there is a pre-processing phase of retinal images in order to filter the noise and then to allow the following extraction of blood vessels. While the method in [1], after the segmentation of retinal image, detects directly the skeleton

vessels and then their bifurcation points, this method proceeds with the application of a genetic algorithm for border extraction, skeleton process and, at the end, utilises a tracking algorithm to obtain retinal strategic points. By means of this technique it is possible to avoid the loss of several particulars of images using the information given from edges that allow to characterise also the bifurcation points obtained from the crossing of thinner vessels. These further steps enable to achieve a number of points that allow an efficient personal identification process.

A database of 12 images containing 256 grey levels has been used for elaborations. The used digital medical images have been acquired with fluorescent angiography and, moreover, have a resolution of 512 x 512 pixels and a quantization of 8 bit per pixel. An example of used images is depicted in Figure 1.

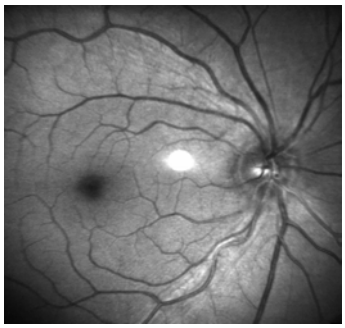

Figure 1. Retinal fundus image.

2. VASCULATURE EXTRACTION

In the first step of this process is used a combination of algorithms, existing in literature [1], for retinal features extraction. The output of this stage is a correct representation of vasculature without loss or alteration of image particulars.

2.1 Pre-processing

The characteristic of retinal fundus images is to have the same grey levels both for backgrounds and vasculature. This problem is due to the presence of impulsive noise given by the acquisition tools and of structural noise given by the anatomic shape of the retinal fundus. For these reasons, to characterise the searched retinal features, it is necessary a good image pre-processing. It is realised making uniform the image by using the same retinal non-linear features. This pre-processing technique consists of a strong compactness operation of grey levels where classic thresholds systems fail because of loss of a large number of important particulars.

The applied filter answering to our necessity, famous in literature with the name of Naka-Rushton filter [10], is regulated by the law:

$$O(i,j) = \frac{I(i,j)}{I(i,j) + \mu_{window}}$$

where *O(i,j)* is the output matrix, that is the transformation result, *I(i,j)* is the elaborated image matrix and μ_{window} is the media of pixels in the choice exploration window.

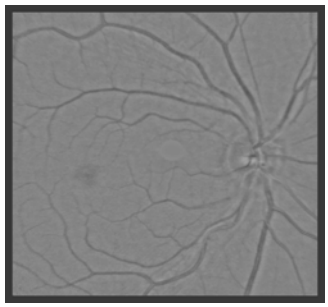

Figure 2. Image after Naka-Rushton filtering.

The result of this process, an image with a greater contrast between background and objects, is depicted in Figure 2.

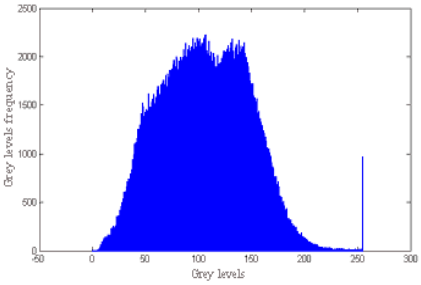

Figure 3. Original image histogram.

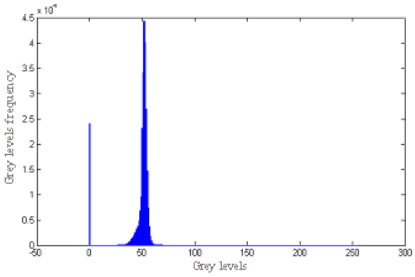

Figure 4. Retinal fundus image histogram after Naka-Rushton filtering.

The filter action is an equalization of grey levels and this operation is more visible looking histograms of original image and image after filtering (see rispectly Figure 3 and Figure 4).

2.2 Vasculature identification

The image, after pre-processing, is filtered to extract vasculature with a clustering of image [6]. The two clusters in which image is split on, are vasculature cluster and background cluster. It is an iterative method that uses average and standard deviation to start and Mikowski distance to distinguish pixels of vasculature from background.

The output image has two levels: black pixels and white pixels that are respectively the vasculature and background (see Figure 5). In the image, now, it is present an impulsive noise. By a successive application of morphological operators of erosion (see Figure 6) and dilation first (see Figure 7), and median filtering after (see Figure 8), it is obtained an image in which noise is reduced and features are preserved.

In particular, the operations of erosion and dilation use hyperbole filter [3] [4] [9], in the first case on negative image with a window of 17 x 17 pixels and in the second on image with a window of 3 x 3 pixels.

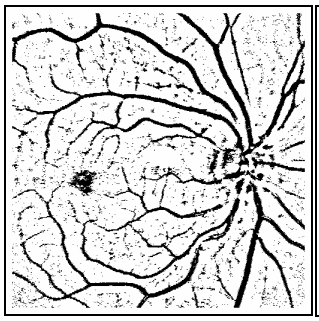

Figure 5. Clustered image.

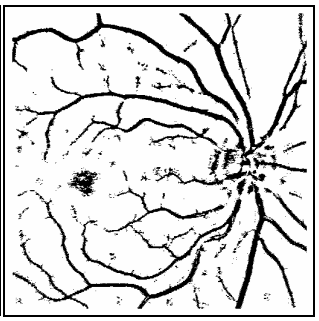

Figure 6. Erosion operator on negative of Figure 5.

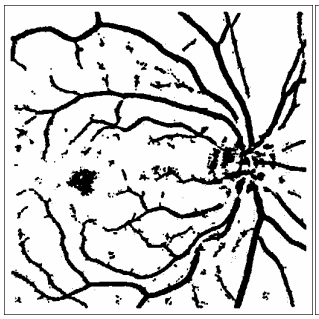

Figure 7. Dilation operator on Figure 6.

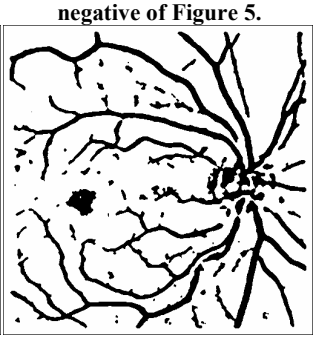

Figure 8. Image after median filtering.

3. GENETIC ALGORITHM FOR EDGE EXTRACTION

The vessel edge detection, existing in literature [2] [3], is performed by using a genetic approach in which the problem is formulated as one of function cost minimization. In particular has been chosen an edge detection algorithm by which it is possible to preserve some properties of the vessels edges looked for. The semantic interpretation and recognition of the observed object have found on the edge detection, understanding the sequences of disposed edges so that to form closed lines with this term, possibly deprived of gaps and blind ramifications.

The search of the optimal solution to the objective function, is performed through an iterative procedure applied to a population of chromosome corresponding to feasible solutions to the problem. The genetic algorithm implements a multi-directional search maintaining a population of potential solutions and encouraging the exchange of information between themselves. The adopted cost function is that proposed by Tan for the measure of edge fitness from real images. It introduces a cost factor related to the correct localization of edges based on a criterion of difference between adjacent regions [5].

The point cost of a binary edges image S at the position p = (i,j) is obtained like weighted sum of opportune cost factors:

$$F(S,p) = \sum_i W_i C_i(S,p)$$

The total cost F (S) of an edges image S is given by adding of the point cost at each pixel of the image:

$$F(S) = \sum_p F(S,p)$$

Therefore, considering two edge images S_a and S_b identical everywhere less that in a 3 x 3 pixel region with centre on the p position, a comparative cost function could be defined as follows:

$$\Delta F = (S_a, S_b, p) = \sum_{I(p)} \sum_k W_k [C_k(S_a,p) - C_k(S_b,p)] = \sum_{I(p)} \sum_k \Delta C_k(S_a, S_b, p)$$

where $0<=C_k<=1$ and $W_k>=0$. The C_k terms are the factors of cost and the W_k terms the relative weights. With these positions, if F (S_a, S_b, p)<0, S_a corresponds to a configuration of edges better than S_b, while it is the contrary when F (S_a, S_b, p)>0. If F (S_a, S_b, p)=0 the two configurations are equivalent in terms of cost. Relatively to the C_t costs, C_c and C_f, the local attribute means the exclusive dependence of such factors from the configuration assumed from the contours in an about 3 x 3 of the pixel observed, while C_d depends only from the value assumed in the observed position (i,j) from the image D of the dissimilarities, that is calculated processing the image of dissimilarities by means of a template-matching with suppression of the not maxima. The C_d cost is to emphasise those pixels that constitute the common boundary between different adjacent regions and to introduce a penalty for those pixels not yet labelled like edge. Therefore the image D of the dissimilarities must have a real value in each p position in the interval [0,1] (0 for no difference, 1 for maximum difference) proportional to the degree of dissimilarity between adjacent regions in that point. In order to derive this image, it is necessary to fix, first of all, a base of edge structures locally valid and, for each element of such base, the form of the two regions R_1 and R_2 on the opposite sides of the structure from whose difference C_d will depend on; therefore it is necessary to fix a function f(R_1, R_2) for the calculus of the dissimilarities. In this case, the whole of the 12 principal edge locally valid (see Figure 9), has been adopted like base, being all constituted by 2 edge pixel, beyond to the central pixel always present, disposed in a square window 3 x 3 or in line (4 combinations) or in way from to the more an angle of bending of 45° (8 combinations).

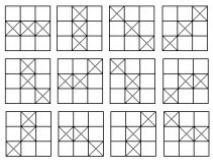

Figure 9. The 12 main locally valid edge structures.

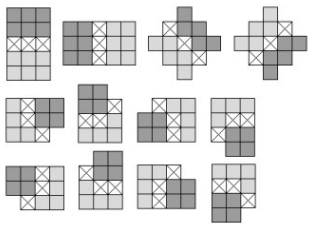

Figure 10. The regions to evaluate dissimilarities measure.

Concerning the function to evaluate dissimilarity function $f(R_1, R_2)$ (see Figure 10), supposing for simplicity to investigate only the extraction of edge obtained from the discontinuity of grey level (step edges), this has been fixed like difference between the averages of grey levels in the aforesaid two regions of interest.

$$f(R_1,R_2) = \frac{1}{n_1}\sum_{p\in R_1} G(p) - \frac{1}{n_2}\sum_{p\in R_2} G(p)$$

The C_t cost has been introduced to emphasise the contours locally thin, making a penalty for those locally thick. A pixel of contour has to be considered when it involves the existence of multiple connections between two or other pixel in the surrounding about 3 x 3. The C_t cost of a point of edge will come therefore engaged equal to 1 if such point is thick according to the preceding definition, or equal to 0 in contrary case (see Figure 11).

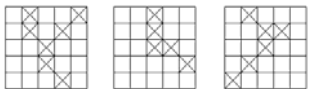

Figure 11. C_t=0, C_t=1, C_t=1.

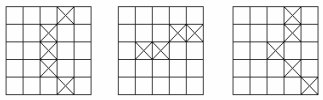

Figure 12. C_c=0, C_c=0.5, C_c=1.

The C_c cost has been introduced to improve the structures of contour locally linear in spite of those locally curve. An edge pixel has to be considered locally not bend, curved or very curved on the average if, always in the window 3x3 surrounding, you have the presence respectively of the 4 linear structures, or of the 8 structures with angle of bending of 45°, or of any other structures. The C_c cost (see Figure 12) is set to 0 for a pixel not curved, 0.5 for a pixel curved on the average, 1 for a very curved pixel.

The C_f cost has been introduced to improve the structures of contour locally continuous in spite of those bended. An edge pixel has to be considered locally not bended, bended on the average, or much bended if, always in the surrounding about 3x3, it has respectively more than a pixel of adjacent contour, an only pixel of adjacent contour, or no pixel of adjacent contour. The C_f cost is therefore set to 0 for a pixel not bended, 0.5 for a pixel bended on the average fragmented, 1 for a pixel much bended (see Figure 13).

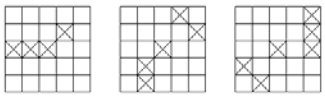

Figure 13. C_f=0, C_f=0.5, C_f=1.

The C_e cost has been introduced to contain the number of pixel labelled like contour, balancing the opposite inherent tendency in the C_d cost. The C_e is set to 0 for a pixel not labelled like contour, to 1 for a pixel labelled like contour. By an opportune decisional tree it is possible to improve the evaluation of the individuals' costs.

Concerning the weights attributed to the costs, Tan suggests a series of values generally valid, but to adapt however of time in time on heuristic base; set C_e = 1.00 follows W_d= 2.00, W_c={ 0.25, 0.50, 0.75}, W_f={ 2.00, 3.00, 4.00} and, in the case in which you want that to the local minima of the cost function corresponds configurations of contours not thick, W_t is set = 2 W_f+ W_d-W_c-W_e.

This algorithm, using an opportune code for the solutions and, above all, thanks to a very efficient pair of mutation strategies, has produced the final edge image depicted in Figure 14.

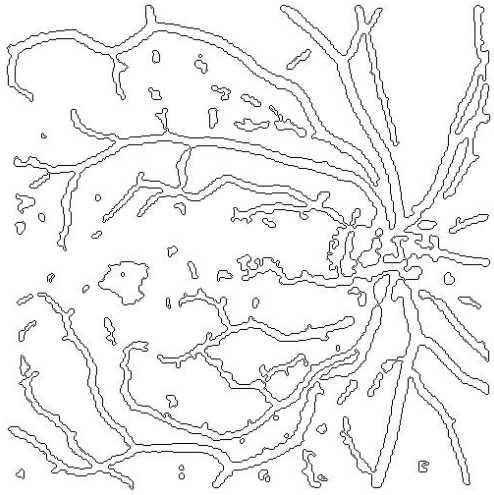

Figure 14. The final edge image.

4. SKELETON PROCESS

The next step consists to realise the skeleton of the blood vessels from the edges template image obtained in the previous phase.

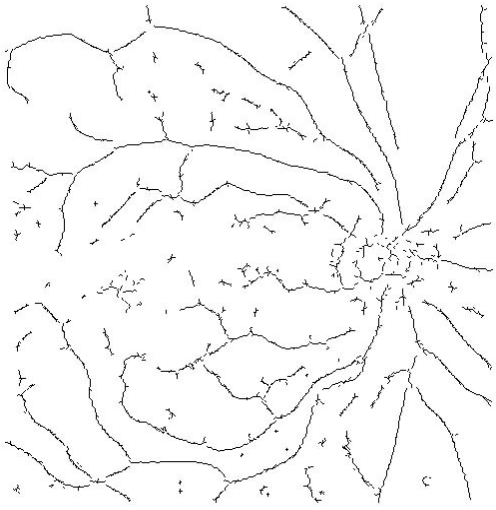

Figure 15. Whole skeleton image.

The skeleton process is divided into two moments: the edges image is processed in the first time in horizontal direction and in the second time in vertical direction. In a few words, considering the images like a matrix of 512 rows and 512 columns, for each row and each column that are met in the vertical and horizontal scansion respectively, all couples of points with a sufficient distance to be considered to belong to the edge of the same vessel, are individuated and for each of them is traced the median point in a output image. In this way, the complete skeleton is produced.

At the end the two images so obtained are fused and the final image is processed in order to clean and eliminate the isolated points (see Figure 15).

5. EXPERIMENTAL RESULTS

After having obtained the blood vessels skeleton, both the image of the edges and skeleton, have been merged in an unique one to exploit, at the same time, the advantages of the information supplied from both the images (see Figure 16). At this point it proceeds with the application of a tracking algorithm that has allowed to characterise the bifurcation points.

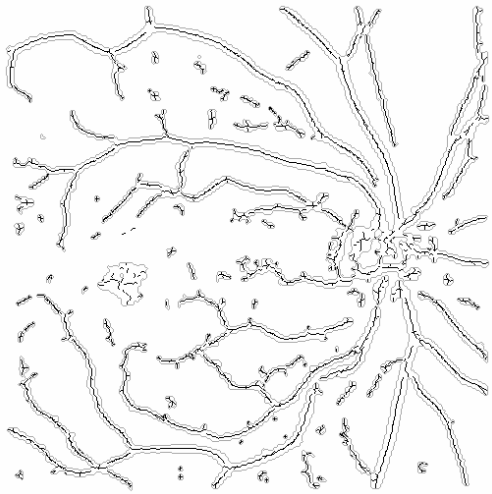

Figure 16. The edge image fused with skeleton image.

In the tracking process the images of width 512 (W in Figure 17) pixels and height 512 (H in Figure 17) pixels, is divided into overlapping blocks of height 32 (L in Figure 17) and width 512 (W in Figure 17). The amount of overlap between consecutives blocks is 16 pixels (P in Figure 17).

The idea of the algorithm is to start from the skeleton and to consider all the couples of points belonging to two parallel vessels that, at the end of their way, could converge forward a bifurcation point.

When a couple of this type is characterised, the tracking process starts with the pursuit of the points of the vessels contour under examination and, in particular, following the way covered by those edge points that are between the two skeleton points (see Figure 18).

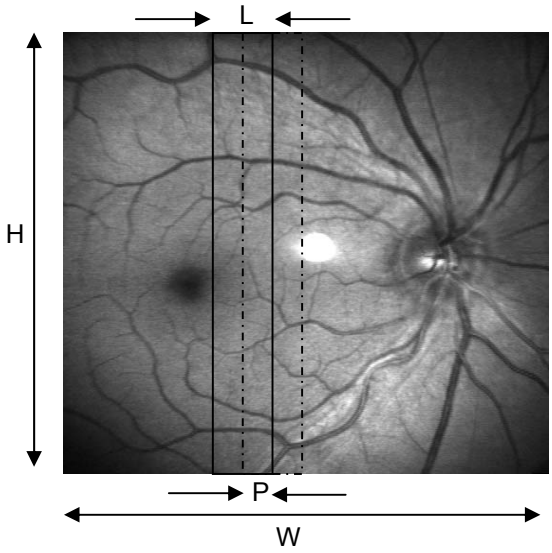

Figure 17. Retinal image parameterisation and blocks extraction.

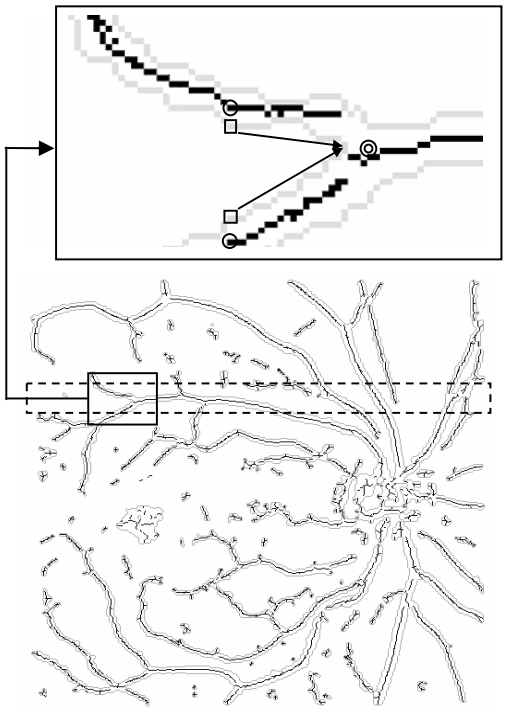

Figure 18. Tracking algorithm process.

Because of the different forms of blood vessels, it has been necessary to re-propose previous process, analysing the image in all the four directions: from left to right, from right to left, from top to down, from bottom to up, in order to cover all the bifurcation and crossover points characterised by two vessels coming from different directions (see Figure 19).

The path of edge points is tracked by matching it, step by step, with preset schemas of routes, that are different for each of four scanning directions (see Figure 20).

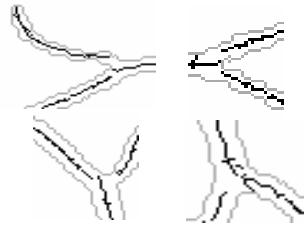

Figure 19. Examples of different forms of blood vessels in the four directions.

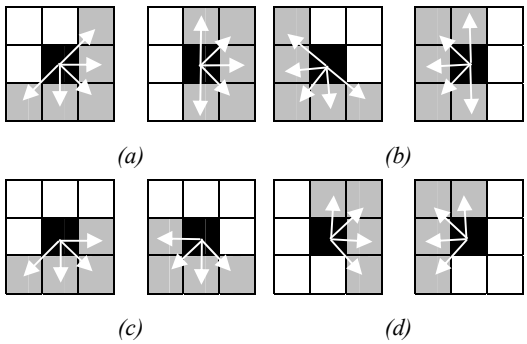

Figure 20. Possible routes of the two edge points considered in scanning (a) from left to right, (b) from right to left, (c) from top to down, (d) from bottom to up.

When these tracked ways join, then a bifurcation point is characterised. The obtained bifurcation and crossover points are depicted in Figure 21.

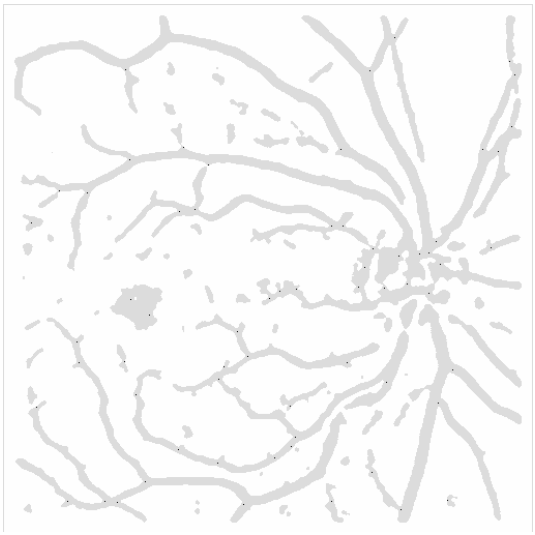

Figure 21. The obtained bifurcation and crossover points.

Although the number of points achieved by this features extraction process is not complete, it allows an efficient and sure personal identification process. In fact, this method has been tested using a database of 12 images containing 256 grey levels, obtained by an oculistic clinic of a local hospital. This database is formed by images of 11 different persons, where two images belong to the same person. The present method has been applied on all images of the database, obtaining, for each of them, a bifurcation and crossover points template. The matching of this templates has allowed to perform an efficient and correct identification of the two images that in 12 images database belong to the same person.

6. REFERENCES

[1] Bevilacqua, V., Cambò, S., Cariello, L., and Mastronardi, G., *A combined method to detect retinal fundus features*, Proceedings of IEEE European Conference on Emergent Aspects in Clinical Data Analysis (EACDA), Pisa (Italy), paper No. 13, 2005.

[2] Bevilacqua ,V., Cariello, L., Introna, F., Mastronardi, G., 2005, *A Genetic Algorithm Approach to Detect Eye Fundus Vessel Bifurcation Points*, Proceedings of Int. Conference, CIMED'2005, Lisbon ISBN 0-86341-520-2, pp.355-360.

[3] Bevilacqua, V., Mastronardi, G., *Edge detection using a Steady State Genetic Algorithm*, Proceedings 16th IMACS World Congress 2000 on Scientific Computation, Applied Mathematics and Simulation, Losanna ISBN 3-9522075-1-9, paper No. 215-8, 2000.

[4] Bevilacqua, V., Mastronardi, G., *Image segmentation using a genetic algorithm*, Proceedings of Int. Conference on Advances in Soft Computing, Physica-Verlag ISSN 16153871, ISBN 3-7908-1544-6, Springer-Verlag, pp. 111-123, 2002.

[5] Bevilacqua, V., Mastronardi, G., Colaninno, A., D'Addabbo, A., *Retina Images Processing Using Genetic Algorithm and Maximum Likelihood Method*, Proceedings of Int. Conference ACST 2004, Advances in Computer Science and Technology, Virgin Islands, USA, pp. 277-280, 2004.

[6] Hsu, W., Pallawa, P.M.D.S., Lee, M. L., and Eong, K. A, *The Role of Domain Knowledge in the Detection of Retinal Hard Exudates*, CVPR, IEEE, vol. 2, pp. 246-251, 2001.

[7] Jain, A.K., Ross, A., Prabhakar, S., *An Introduction to Biometric Recognition*, IEEE Trans. on Circuits and Systems for Video Technology, Vol. 14, No. 1, pp 4-19, January 2004.

[8] Kresimir, D.I , Mislav, G., *A Survey of Biometric Recognition Methods,* 46th International SyrnPoSium Electronics in Marine, ELMAR-2004, Zadar, Croatia, 16-18 June 2004.

[9] Marino, F., and Mastronardi, G., *Hy2: A Hybrid Segmentation Method*, Proceedings of International Conference IWISP, pp. 311-314, 1996.

[10] Naka, K.I., Rushton, W.A., *S-potentials from Luminosity Units in the Retina of fish (Cyprinidae)*, Journal of Physiology, 185, pp. 587-599, 1966.

[11] Wilson, C.L. and McCabe, R.M., *Simple Test Procedure for Image-based Biometric Verification Systems*. NISTIR 6336, National Institute of Standards and Technology, 1999, http://www.itl.nist.gov/iaui/ 894.03/pubs.htm.